Flow Misalignment and Tidal Stream Turbines

C Frost[#1], PS Evans[#2], CE Morris[#3], A Mason-Jones[#4], D O'Doherty[#5], T O'Doherty[#6]

[#]*School of Engineering,*
Cardiff University,
CF24 3AA
[1]FrostC1@cardiff.ac.uk
[2]Evansps3@cf.ac.uk
[3]MorrisCE3@cardiff.ac.uk
[4]Mason-JonesA@cardiff.ac.uk
[5]OdohertyDM@cf.ac.uk
[6]Odoherty@cf.ac.uk

***Abstract*— Extensive Research and Development (R&D) within the tidal energy industry is pushing this sector towards commercial viability, with full scale prototypes starting to meet the challenges of the marine environment. This paper combines velocity data collected from Ramsey Sound (Pembrokeshire, Wales), with Computational Fluid Dynamics (CFD) to assess the impact of non-rectilinear flows on turbine rotor performance. This requires both the geometry of the turbine and the surrounding free stream velocity to be studied. From the site data, the majority of the velocities tend to fall within a ±20° misalignment to the principle flow direction for velocities greater than the economic viable threshold of 2 ms^{-1}. From the CFD it was found that the non-dimensional performance parameters reduced with increasing angles of misalignment between the axis of rotation and free stream velocity. The resultant magnitude of the bending moments about the head of the driveshaft for the misaligned turbines were found to be up to nine times greater, than the aligned turbine. The paper shows that the tolerance to axial flow misalignment between the free stream velocity and axis of rotation of a turbine requires defining, in order to avoid the detrimental effects it has on performance and loading.**

***Keywords*— TST, CFD, Misalignment, Loading, Performance**

I. Tidal Energy

Tidal energy technology has been gaining momentum in recent years, particularly in the UK, which has a vast coastline. The predictable nature of tidal energy allows for regular electrical generation at higher power densities than other renewable energy resources [1]. Several studies [2][3] have highlighted areas with the greatest power density from tidal stream energy based on the available power, including the Pentland Firth in Scotland. However the extractable resource must also be considered and this will be the focus of the following section.

The characterisation of the flow field at a potential tidal energy site is crucial in predicting the performance of a device in its true environment. A study of Ramsey Sound in Pembrokeshire, South Wales has been made [4]. The field data includes velocity measurements, collected from Ramsey Sound. The data has identified the presence of flow misalignment from the principle flow direction, which travels north through the sound, during the flood phase of the tide [5][6].

The misalignment angle from the axial flow axis is considered important from a turbine performance, capacity factor and structural loading perspective as highlighted by Harding and Bryden [7]. Many Tidal Stream Turbine (TST) designs rely on near uni-directional flows and are therefore relatively unresponsive to small deviations in directionality [7] Deviations from the axial plane can compromise the performance of horizontal-axis TSTs [8]. Furthermore, this is reinforced by Easton et al. [9] who noted that these flow features could significantly affect a TST's operational efficiency.

In Ramsey Sound, the majority of the velocities tend to fall within the ±20° tolerance, as suggested by Harding & Bryden [7] and shown in Figure 1. It can be seen that velocities greater than the economic viable threshold of 2 ms^{-1} will predominantly fall within the principal flow axis ±20°. The bathymetry and coastline configuration are highly influential on both the flow magnitude and direction. Away from the central portion of the Sound, the velocities are acted upon by various promontories, reefs and shelving areas, which deflect and retard the flow. This results in a deviation of the flow away from the principle flow direction of greater than 20° at lower velocities, particularly towards the outer edges of the Sound.

II. Tidal Stream turbines

Quantifying an acceptable misalignment angle is difficult. The effect of directionality is dependent on a variety of factors, including the type of tidal energy device being installed. It is therefore important to establish the tolerance to misalignment of a TST if the device has a fixed orientation, and is unable to extract energy from all directions. It is also important to know the impact of misalignment in order to identify when a device would benefit from yawing to maintain within these tolerances.

Of the numerous devices in development at the European Marine Energy Centre, EMEC [10] and other development sites across the UK, the majority of TSTs, can be separated into two groups. The first group of devices includes those devices which have a fixed direction that depend on the tides bi-directionality (ebb flow direction at 180° from flood flow direction) to generate on both phases of the tide; these include such devices as MCT – Seagen and OpenHydro. The second group include a yaw mechanism which allows the rotating plane of the turbine to be maintained perpendicular to the flow; such devices include Alstom and TEL Ltd devices [10].

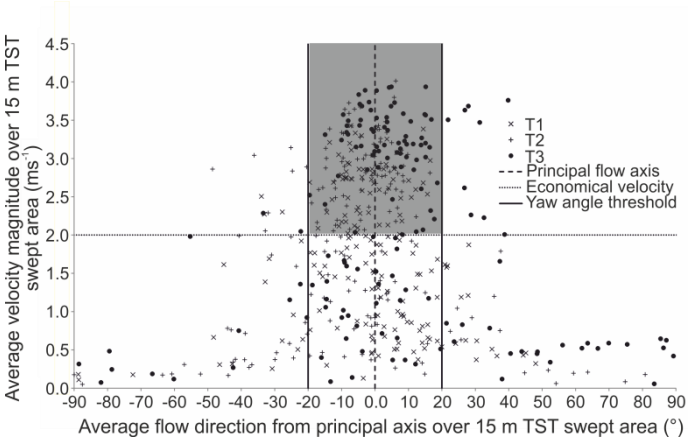

Figure 1. Plots of average velocity magnitude (resultant of $\bar{u}$, $\bar{v}$ velocity components) over a 15 m TST swept area along transects T1 – T3 as a function of the average incident flow angle during peak flood [4].

In both these cases the issue of axial flow misalignment must be considered. For the former of these two groups, they have other systems in place such as 180° pitching of the blades and drive trains designed to operate with thrust loads onto the shaft as well as loads pulling the rotor off the shaft. It is however necessary to know how varying angles of axial flow misalignment will impact its performance. The same study is necessary for the latter group also as it may not be economically justifiable or possible to actively track the incoming flow and align the turbine perpendicular to it continuously. Whilst yawing can be utilised to counter some misalignment it must be recognised that it is limited. Actively tracking a rapidly varying misalignment is both economically and mechanically unlikely.

The aim of this work therefore is to inform the sector and device designers of this potential issue and make recommendations based on numerical modelling of various misalignment scenarios. This will be done by characterising the performance of a TST, for various angles of axial flow misalignment. From the results shown in Figure 1 and previous work [4][11] a 20̊ tolerance was set for the misalignment at the boundaries of the CFD models. This agrees with other site data as found by Harding & Bryden [12]. The non-dimensional performance characteristics, resultant bending moments and the angle at which they act for a 10m diameter TST were determined. Both the experimental model at lab scale, the CFD model at lab scale and the full scale CFD model (10m diameter) have strong agreement of their non-dimensional performance characteristics as shown from previous work [13]. This previous work provides confidence, in the performance characteristics, for uniform and profiled flow in an aligned turbine case. Characterisation of the performance was determined using ANSYS CFX at 10° increments from the 0°, aligned turbine, up to 20° misalignment. The sign convention for the angle of misalignment along with the turbine and support structure used in this study can be seen in Figure 2. Only the positive angles of misalignment have been considered in this paper.

III. Numerical Model

The support structure was formed from a tripod supporting the central load bearing stanchion as can be seen in Figure 2. The turbine's axis of rotation was aligned to the centre of the rotational domain and the geometry fell within its boundaries so as to avoid blockage effects from the side walls. The geometry specifications for the turbine are given in Table 1. The turbine has been modified from previous studies to enhance performance at the root of the blade by removing the previous pin connection and blending the blade with the hub. The turbine was expected to have similar non-dimensional performance characteristics to the well documented geometry of the previous turbine [11][13] .

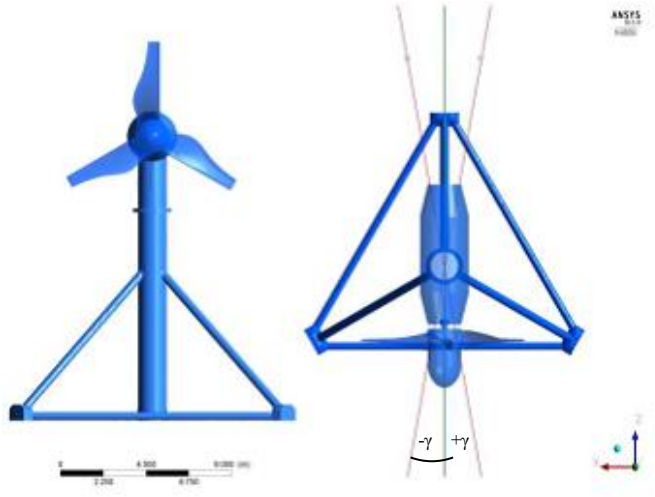

Figure 2. TST and support structure with misalignment sign convention

The rotational axis of the turbine and the central axis of the rotational domain were axially aligned in all cases and were maintained parallel to the horizontal plane of the domain, 15m above the seabed and 45m below the top surface of the domain. The axis was then rotated about the centre of the stanchion, to produce the misaligned cases, as can be seen in Figure 2.

TABLE I.
TURBINE GEOMETRY

Turbine Specification:	Value:
Turbine diameter (D)	10 (m)
Hub diameter	1.8 (m)
Blade profile	Wortmann FX 63-137
Blade twist (root to tip)	33 (°)
Optimum blade pitch	6 (°)
Stanchion diameter	1.8 (m)
Nacelle diameter	2.6 (m)
Tower width	15 (m)
Tower height	15 (m)

The total number of elements in the domains reached circa 9 million tetrahedral elements. Specific concentration of the mesh was applied about the tips of the blades, the blade root and hub as well as within the rotational domain of the turbine. The sea domain consisted of 7 million elements and the rotating domain 2 million elements. These mesh parameters were maintained for all cases of misalignment.

From the results, the non-dimensional performance characteristics and Tip Speed Ratio (TSR) could be determined using equations 1-4 for coefficient of power C_P, coefficient of Torque C_θ, coefficient of Thrust C_T, and TSR respectively as defined by Mason-Jones, et al [15].

$$C_P = \frac{T\omega}{{}^1/_2 \rho A V^3} \quad (1)$$

$$C_\theta = \frac{T}{{}^1/_2 \rho A R V^2} \quad (2)$$

$$C_T = \frac{F}{{}^1/_2 \rho A V^2} \quad (3)$$

$$\text{TSR} = \frac{\omega R}{V} \quad (4)$$

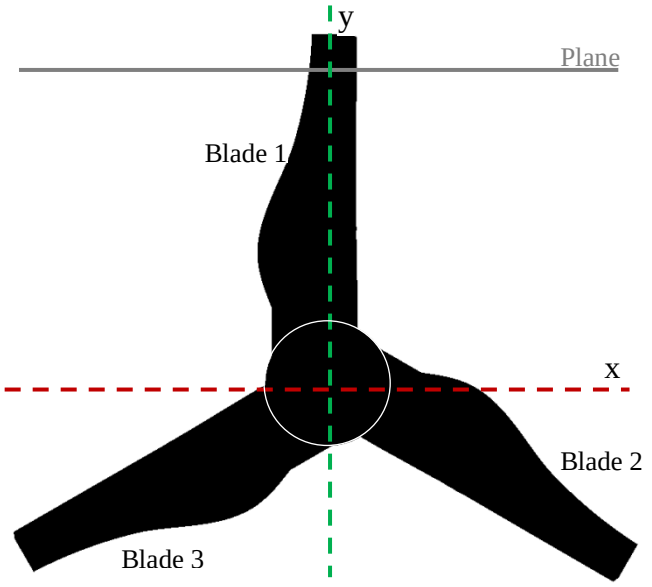

Figure 3 Axis about which the bending moments are taken.

Previous work [13][14] looked at the effect of clearance between a stanchion and the turbine on the shaft bending moments of a turbine. The bending moments are calculated by taking the torques about the x and y axis of the turbine, as seen in Figure 3.

IV. RESULTS

The data output from ANSYS CFX was post processed in order to obtain the direct torque, thrust and bending moments for each of the blades and the hub. These were then used to calculate the performance characteristics, C_P, C_T and C_θ against TSR using equations 1-4. The same area and free stream velocity were used to calculate the non-dimensional performance characteristics of the misaligned turbines as for the aligned turbine. This was done to make the results comparable, even though the theoretical maximum power will have changed as the projected area of the turbine has changed to an ellipse. Resultant magnitude of bending moments and angle at which these moments act were also calculated.

Figure 4 shows the C_P of an aligned TST against axial misalignments of γ= +10° and +20° for increasing Tip Speed Ratios (TSRs). The aligned turbine has a peak C_P of 0.43, at a TSR of 3.6 and hits freewheeling at a TSR of approximately 6.8. The 10° misaligned turbine has a very similar performance up to a TSR of about 2, after which the performance curve begins to diverge slightly to a lower peak C_P of 0.40 at a slightly lower TSR of 3.5, the 10° misaligned turbine reaches freewheeling at a TSR of 6.7, slightly lower than the aligned turbine. The final sets of points on the curve are from the 20° misaligned turbine and show significant differences. Whilst up to a TSR of 2 the points appear to match the aligned and 10° cases, after this point the 20° curve diverges significantly, the peak C_P value of 0.32 now occurring at a lower TSR of 3. These significant changes in the C_P between the aligned case, 10° misaligned case and the 20° misaligned case shows there is a non-linear relation between the effects of misalignment and the turbine performance. This is supported by considering the percentage drop in C_P performance, at peak power for the aligned turbine (TSR=3.6) there is a 7.5% drop in performance to the 10° misaligned case, however from the aligned to the 20° misaligned case there is a 29% drop in C_P performance. The drop in C_P between the aligned case and both misaligned cases was expected. The percentage change in peak power between 10° and 20° misalignment and the aligned case shows it is not

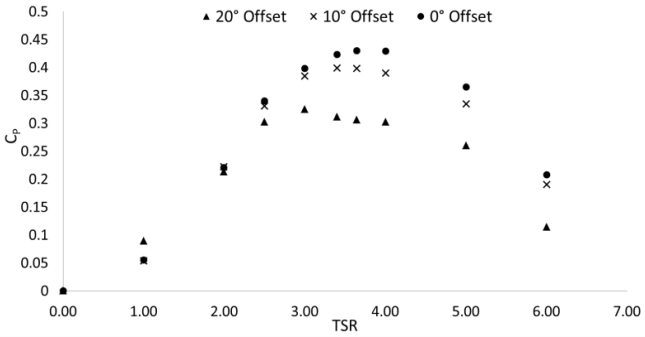

Figure 4. C_P against TSR for turbine misalignments

a linear relationship. The 20° misalignment curve appears to have become truncated with a much flatter peak. In addition the 20° misaligned turbines reach freewheeling at a lower TSR than both the aligned turbine and the 10° misaligned turbine. The aligned and 10° misaligned turbines reach freewheeling at a TSR of 6.8, whilst the 20° misaligned reaches freewheeling at a TSR of 6.5.

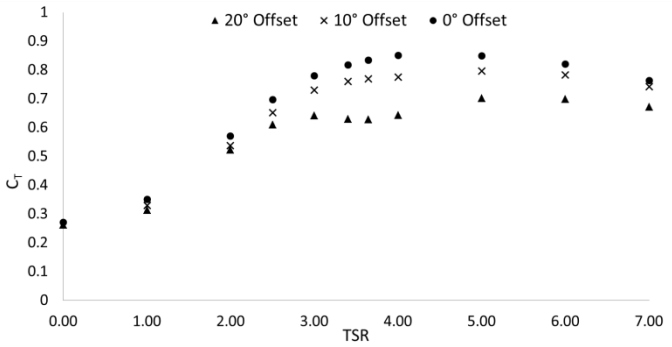

Figure 5. C_T against TSR for turbine misalignments

Figure 5 shows the C_T, acting on the rotor against TSR for the three cases. It can be observed that the greatest C_T values occur in the aligned case with peak C_T of 0.85 occurring at a TSR of 4. The C_T of the 10° misaligned case peaks at a higher TSR of 5 with a value of 0.78 whilst the 20° misaligned case also peaks at a TSR of 5 but at a significantly lower value of 0.70. In addition to the latter and lower curve, the 20° misaligned turbine also has a drop in thrust between a TSR of 3 and 4. The percentage drop in peak thrust for the aligned case is similar to the percentage drop seen in C_P. The 10° misaligned turbine is 9% lower and the 20° misaligned turbine is 24.5% lower than the aligned turbine. The shape of the curves however does remain similar with a slight dip in the 20° misaligned case, between a TSR of 3 and 4.

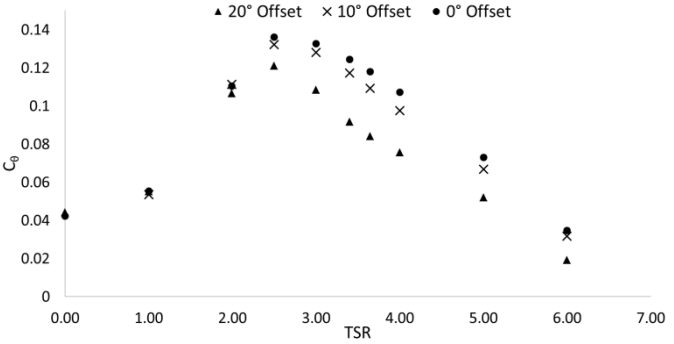

Figure 6. C_θ against TSR for turbine misalignment

Figure 6 has a comparison of the coefficient of torque, C_θ for the three cases. The aligned turbine has a peak C_θ at TSR of 2.5, with a value of 0.136. For the 10° misaligned turbine there is a 3% drop in performance at peak C_θ which remains near TSR of 2.5, the C_θ value is now 0.132. There is an 11% drop between the aligned turbine and 20° misaligned turbine; with a C_θ value of 0.121. The curves do not diverge until close to the peak with the 20° case peaking lower than the others, the general shapes of the curves are very similar overall.

Figure 7 shows the magnitude of resultant bending moments which was taken about the head of the driveshaft ie the rotor end. As can clearly be seen, in this blade orientation with blade 1 at top dead centre TDC, there is a significant increase in the bending moment with the inclusion of axial misalignment. The aligned turbine experiences a peak bending moment of 16 kNm at a TSR of 3. This agrees with previous work [16] whilst the bending moment for the 10° misaligned turbine peaks at a TSR of 5 with a magnitude of 80 kNm. The bending moment for the 20° misaligned turbine also peaks at a TSR of 5, with a significantly higher magnitude of 150 kNm. These extreme increases in the magnitude of resultant bending moment are of concern and need further discussion. The pattern in the magnitude initially shows an increase in magnitude as the TSR increases, however the figure then shows a dip in magnitude for the 20° misaligned turbine as it increases to a TSR of 4. The 20° misaligned turbine then rapidly rises to a peak bending moment of 150 kNm at a TSR of 5, before receding again. The same pattern applies to the 10° misaligned turbine however the drop is less prominent at TSR of 4 and the rise to peak less at a TSR of 5.

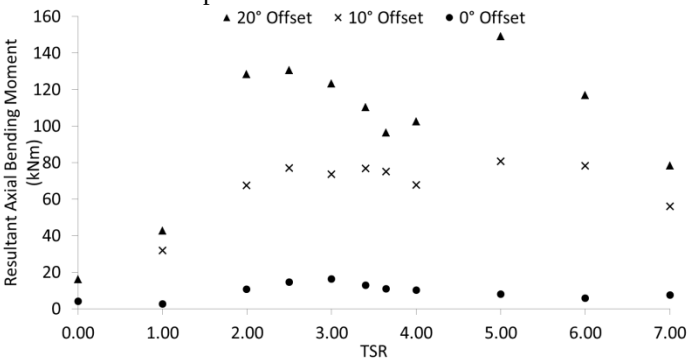

Figure 7. Resultant magnitude of bending moment about the driveshaft of the turbine against TSR for turbine misalignments

Figure 8 shows the angle at which the resultant bending moment is acting; lines have been included to help follow the trend. It can be seen that there are similarities between the two misaligned turbine cases. However without further transient data to see the effect of blade position as well, it is difficult to pick out the correlation to increasing the TSR and therefore further work to determine the relationship between angle of acting bending moment and misalignment is required.

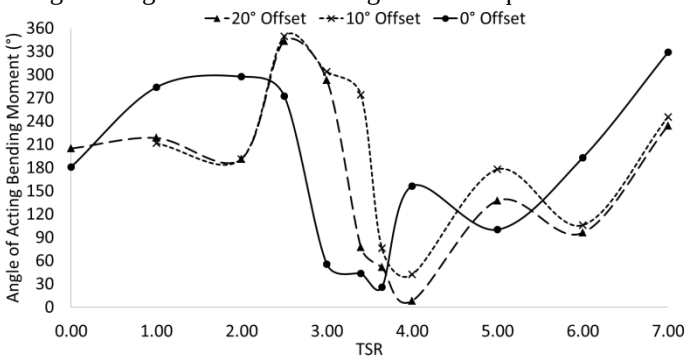

Figure 8. Angle of acting bending moment about the drive shaft of the turbine against TSR for turbine misalignment

Figure 9 shows the pressure contours about Blade1 for three TSR values and various angles of turbine misalignment. The plane on which these pressure contours were taken is shown in Figure 3. What is shown from these plots is that the breakdown of the pressure contours near the tip of the blade occurs as the relative velocity at the tips of the turbine blades increases. The contours for a TSR of 2 are all very similar with a high pressure region on the front face of the blade (the bottom face in Figure 9) and a low pressure region on the back face of the blade. There is a slight change however as the TSR increases to 3.65, which is close to peak power. It can now be seen that a low pressure region has begun to form on the front face of the blade. The low pressure region is small for the aligned and 10° misaligned turbines, but is considerably larger for the 20° misaligned turbine. As the turbines approach freewheeling, the low pressure region on the front edge of the blade can be seen to have increased significantly. The greater the angle of misalignment and larger the low pressure region becomes as it approaches the leading edge of the turbine.

V. DISCUSSION

The performance characteristics for the aligned turbine are in close agreement with previous studies [11][13]. The effect of misalignment on the performance characteristics of the turbine are significant, however the relationship does not appear to be linear. The detrimental effects of misalignment increase considerably, between 10° and 20° turbine misalignments. Whilst an increase in misalignment was expected to cause detrimental effects to performance the relationship appears to be non-linear, however further angles of misalignment will be required to characterise the relationship for this turbine. The peak C_P is reduced with increasing turbine misalignment and the curve is shifted to the left, peaking at a lower TSR. The reason for this reduction in C_θ and thus C_P, is due to the blades' relative angle of attack. At TSRs below 2.5 the effect of the relative angle of attack is not sufficiently noticeable thus the non-dimensional performance curves are similar. The 20° misaligned turbine reaches its stall point at a lower TSR than the 10° misaligned or aligned turbine causing the deviation in C_θ and C_P to occur at TSR above 2.5. This is shown to be the case from Figure 9, however further investigation is required to look at the performance of the blades throughout their

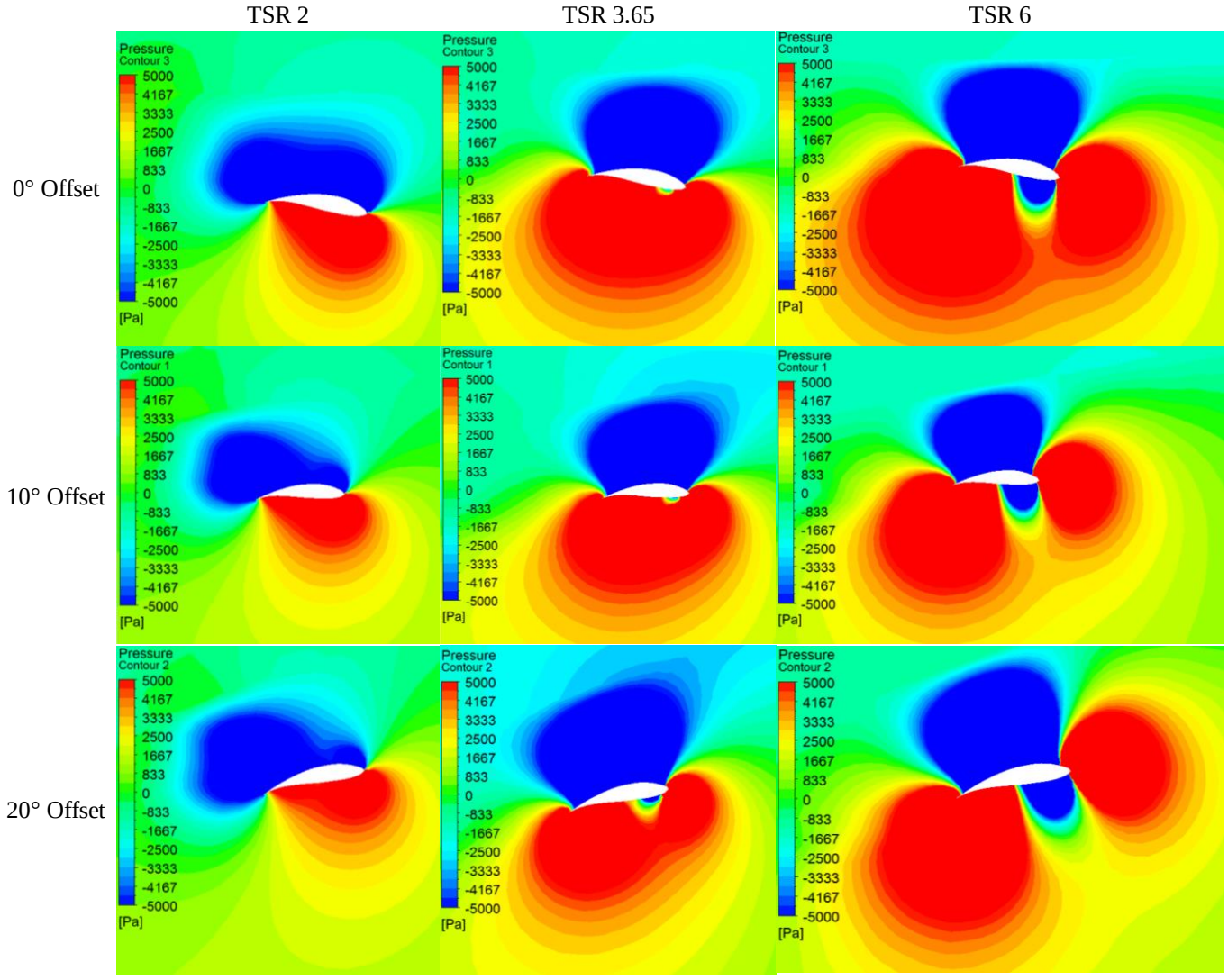

Figure 9. Pressure contours around Blade 1 at 4.5m above the axis of rotation.

rotational path. The thrust is also reduced in the axial direction (but increased side loading will occur) as less of the free stream velocity which imparts the axial thrust force is aligned to the axis, hence thrust shedding occurs.

The impact on the magnitude of bending moment is more significant with the peak magnitude increasing to five times greater for the 10° misaligned turbine and nine times greater for the 20° misaligned turbine, when compared with the aligned turbine. The pattern of the magnitude of bending moment curve (Fig 7) with a dip near peak C_P is due to a reduction in the imbalance, as the moments acting about the x and y axes recede. These values however are a snapshot in the rotation and may not represent the peak magnitude. In order to capture the full effect, transient simulations are required; this will be done in future work.

The effects identified in this paper are likely to be turbine specific and correlated to the blade design, particularly the angle of attack and amount of twist presented along the blade; however this would require further work to establish.

VI. CONCLUSIONS

The numerical modelling has shown that tidal turbines are adversely affected by the misalignment between their axis of rotation and the free stream velocity.

An axial flow misalignment of +10° results in a 7.5% reduction in peak C_P, 3% in peak C_θ and 9% in peak C_T, compared to the aligned turbine. The +20° misaligned turbine experienced a drop of 29% in peak C_P, 11% in peak C_θ and 24.5% in peak C_T, compared to the aligned turbine. The resultant magnitude of the bending moments about the head of the driveshaft for the 10° and 20° misaligned turbines were found to be five times and nine times greater, respectively, than the aligned turbine.

The relationship between turbine performance and axial flow misalignment is not linear and the rapid reduction in performance that occurs between the 10° and 20° misaligned turbines suggests an exponential relationship. However further angles of misalignment will need to be considered to confirm this.

It is clear, that such misalignment between the axis of rotation and free stream flow will reduce the overall performance of a turbine and will reduce the life expectancy or maintenance period of a turbine. The increased loading on the shaft and bearings will increase the likelihood of failure in the shaft support bearings and potentially the gearbox.

The paper has shown that the tolerance to axial flow misalignment between the free stream velocity and axis of rotation of a TST requires defining, in order to avoid the clearly outlined detrimental effects it has on performance and loading.

VII. ACKNOWLEDGMENT

The authors wish to acknowledge the financial support of LCRI and EPSRC SuperGen Marine Grand Challenge. As well as HPCW for use of their high performance computing facilities.

VIII. REFERENCES

[1] Bahaj, A.S., Myers, L., 2004. Analytical estimates of the energy yield potential from the Alderney Race (Channel Islands) using marine current energy converters. Renewable Energy 29 , pp. 1931-1945.

[2] Sustainable Development Commission. 2007. Turning the tide: Tidal power in the UK

[3] Crown Estate. 2013. UK wave and tidal resource areas project. Summary Report

[4] Evans, P., Armstrong, S., Wilson, C., Fairley, I., Wooldridge, C. F. and Masters, I. 2013. Characterisation of a highly energetic tidal energy site with specific reference to hydrodynamics and bathymetry. In: Proceedings of the 10th European Wave and Tidal Energy Conference (EWTEC). 2nd – 4th September 2013, Aalborg, Denmark.

[5] Fraenkel, P.L., 2006, Marine current turbines: pioneering the development of the marine kinetic energy converters. Proc. IMechE Vol. 221 Part A: Journal of Power and Energy

[6] 3 Black and Veatch, 2005. Tidal stream energy resource and technology summary report, Carbon Trust

[7] Harding, S. F. and Bryden, I. G. 2012. Directionality in prospective Northern UK tidal current energy deployment sites. Renewable Energy 44, pp. 474-477.

[8] Batten WMJ, Bahaj AS, Molland AF, Chaplin JR. 2007. Experimentally validated numerical method for the hydrodynamic design of horizontal axis tidal turbines. Ocean Engineering 2007;34(7). ISSN: 00298018:1013e20. doi:10. 1016/j.oceaneng.2006.04.008.

[9] Easton, M. C., Woolf, D. K. and Pans, S. 2010. An operational hydrodynamic model of a key tidal-energy site: Inner Sound of Stroma, Pentland Firth (Scotland, UK). In: Proceedings of the 3rd International Conference on Ocean Energy (ICOE). 6th – 8 th October 2010, Bilbao, Spain.

[10] EMEC (2015) Tidal Developers Page. [Online]. Available: http://www.emec.org.uk/marine-energy/tidal-developers/

[11] Frost, CH. Evans, PS. Morris, CE. Mason-Jones, A. O'Doherty, T. O'Doherty, DM. 2014. The Effect of Axial Flow Misalignment on Tidal Turbine Performance. Renew 2014. Portugal, Conference Proceedings.

[12] DTI, 2007. Economic viability of a simple tidal stream energy capture device. DTI project No. TP/3/ERG/6/1/15527/REP URN 07/575

[13] Mason-Jones. A, O'Doherty. DM, Morris. CE, O'Doherty. T, Byrne. CB, Prickett. PW, Grosvenor. RI, et al. 2012. Influence of a velocity profile & support structure on tidal stream turbine performance. Renewable Energy, 52 (2013) 23-30 ISSN 0960-1481 10.1016/j.renene.2012.10.022

[14] Morris, CE. 2014. Influence of Solidity on the performance, Swirl Characteristics, Wake Recovery and Blade Deflection of a Horizontal Axis Tidal Turbine. PhD Thesis.

[15] Mason-Jones, A., O'Doherty, DM. Morris, CE. O'Doherty, T. Byrne, CB. Prickett, PW. et al. 2012. Non-dimensional Scaling of tidal stream turbines. Energy Journal. Issue 44 820- 829

[16] Frost, CH. Morris, CE. Mason-Jones, A. O'Doherty, DM. O'Doherty, T. 2014. The Effect of Tidal Flow Directionality on Tidal Turbine Performance Characteristics. Renewable Energy. Volume 78, June 2015, Pages 609–620.